AIP | Review of Scientific Instruments

Comparison of different methods to calibrate torsional spring constant and photodetector for atomic force microscopy friction measurements in air and liquid

Torbjörn Pettersson, Niklas Nordgren, Mark W. Rutland, and Adam Feiler

Citation: Rev. Sci. Instrum. **78**, 093702 (2007); doi: 10.1063/1.2779215
View online: http://dx.doi.org/10.1063/1.2779215
View Table of Contents: http://rsi.aip.org/resource/1/RSINAK/v78/i9
Published by the American Institute of Physics.

Comparison of different methods to calibrate torsional spring constant and photodetector for atomic force microscopy friction measurements in air and liquid

Torbjörn Pettersson,[a),b)] Niklas Nordgren, and Mark W. Rutland[a),c)]
Department of Chemistry, Surface Chemistry, Royal Institute of Technology, Drottning Kristinas Väg 51, SE-100 44 Stockholm, Sweden

Adam Feiler
Department of Physical and Analytical Chemistry, Surface Biotechnology, Uppsala University, P.O. Box 577, SE-751 23 Uppsala, Sweden

(Received 6 February 2007; accepted 11 August 2007; published online 5 September 2007; publisher error corrected 23 February 2009)

A number of atomic force microscopy cantilevers have been exhaustively calibrated by a number of techniques to obtain both normal and frictional force constants to evaluate the relative accuracy of the different methods. These were of either direct or indirect character—the latter relies on cantilever resonant frequencies. The so-called Sader [Rev. Sci. Instrum. **70**, 3967 (1999)] and Cleveland [Rev. Sci. Instrum. **64**, 403 (1993)] techniques are compared for the normal force constant calibration and while agreement was good, a systematic difference was observed. For the torsional force constants, all the techniques displayed a certain scatter but the agreement was highly encouraging. By far the simplest technique is that of Sader, and it is suggested in view of this validation that this method should be generally adopted. The issue of the photodetector calibration is also addressed since this is necessary to obtain the cantilever twist from which the torsional force is calculated. Here a technique of obtaining the torsional photodetector sensitivity by combining the direct and indirect methods is proposed. Direct calibration measurements were conducted in liquid as well as air, and a conversion factor was obtained showing that quantitative friction measurements in liquid are equally feasible provided the correct calibration is performed. © *2007 American Institute of Physics.* [DOI: 10.1063/1.2779215]

I. INTRODUCTION

With the rapidly increasing interest in nano- and biotechnology, the ability to quantitatively measure normal and lateral forces at the molecular level has increased in importance. Over the last two decades the atomic force microscope (AFM) has become a routine method for obtaining surface force measurements in air and in liquids with a force sensitivity down to piconewtons. The intrinsic simplicity of measuring the deflection of an AFM cantilever in response to interaction with a surface makes it immediately applicable to a large range of scientific and industrial applications. The development of the colloid probe technique[1] which allows well defined probe geometry and surface chemistry has further increased the usefulness of AFM for use in applied studies.[2]

In many instances the limiting factor in obtaining quantitative force measurements with an atomic force microscope is calibrating the cantilever spring constants and the photodetector sensitivity. In general, the measurement and interpretation of normal forces are simpler to quantify than lateral forces arising from friction largely because the torsional spring constant of AFM cantilevers is harder to calibrate than the normal spring constant. Despite the early application of AFM for friction force measurements, e.g., Refs. 3 and 4, the difficulty in unambiguously determining the torsional spring constant and calibrating the photodetector lateral response meant that this area has not developed as rapidly as, for example, the adhesion and molecular pulling studies. In the last few years the rapid development of microelectrical mechanical systems (MEMSs) with their ever-decreasing size and weight constraint has meant that frictional forces are becoming a pivotal issue. Additionally, the huge interest in molecular engineering and biotechnology in which intermolecular lateral forces dominate the conformation and function of proteins and biomolecules at interfaces has resulted in a desire to quantify these forces.

Over the last few years, many methods have been proposed for calibration of the normal spring constant for AFM cantilevers; these include direct measurement, geometric calculations, and finite element analysis.[5–7] Until recently the method most commonly adopted for normal spring constant determination was based on the measurement of the cantilever's change in resonant frequency in response to added masses.[6] More recently, Sader and co-workers developed equations to calculate the cantilever's normal spring constant from the resonance frequency induced by thermal fluctuations. The method is fast, direct, and requires no functional-

[a)]Authors to whom correspondence should be addressed.
[b)]Electronic mail: bobo1@kth.se
[c)]Electronic mail: mark@kth.se

ization of the cantilever;[7] the use of this method for normal spring constant determination has been increasingly adopted during recent years. Despite a large number of proposed methods,[4,8–14] a single standardized procedure for calibration of the torsional spring constant does not yet seem to have gained general acceptance.[15] For a more detailed review of friction calibration and friction measurements, the reader is referred to a review article by Perry.[16]

Two methods to measure the cantilever torsional spring constant by directly twisting the cantilever have been presented by some of the authors. These two techniques are based on a similar measurement of cantilever normal and lateral deflection but differ by means of applying torque to the cantilever. The pivot method[11] uses a fulcrum based on an upturned cantilever to apply twist, while the lever method[13] utilizes a lever attached to the cantilever to produce twist. The former method is quicker and simpler to apply experimentally and does not compromise the cantilever but is most suited to tipless rectangular cantilevers. The latter method is more demanding experimentally, requiring the gluing of a fiber to the cantilever, perpendicular to its long axis but can be used for any geometries of cantilever with or without tips. Importantly, both calibration methods address the issue of calibrating the photodetector for quantification of the deflection signal. (We note that the wedge method[9] is yet another successful technique for obtaining both torsional constant and photodetector calibration, though a comparison with that method is not within the scope of this work.)

A recent publication has shown that the methods of Sader and co-workers and Cleveland *et al.*[12] can be adapted to calculate the torsional spring constant from the torsional resonant frequency of the cantilever. (These techniques are henceforth referred to as the Sader and Cleveland methods, respectively, according to current praxis.[12]) This development has the potential to provide a standard procedure for torsional spring constant determination with the distinct advantage that the cantilever can be calibrated *in situ* directly prior to force measurement. However, a direct comparison between the calculated torsional spring constant and that derived by direct measurement has not yet been presented. Moreover, calibration of the photodetector also needs to be performed.

In this article we compare values of the torsional spring constant obtained from calculation based on the cantilever resonance with direct measurement due to applied torque. While there is no *a priori* reason to expect a significant difference, no internal comparisons between these static techniques or external comparisons with the dynamic techniques have previously been performed. Since there are several communities using different techniques it is topical to ensure that the data are comparable. Furthermore, if the dynamic and static methods can be shown to be quantitatively in agreement, then the results obtained from these techniques can be reverse engineered to simply obtain a reliable photodetector calibration.[14]

Importantly calibration has been conducted in both air and liquid due to the increasing application of measurements in liquid, and a conversion factor, based on refractive index analysis, is discussed to relate calibration in the different media. In addition, we evaluate the accuracy of calculating the photodetector sensitivity directly from the deflection. Since a value for the normal spring constant is required to obtain the torsional spring constant, we also briefly compare the two above mentioned normal calibration methods for a large number of cantilevers from the same batch.

In brief the salient points in this article are (i) comparison of the dynamic and static friction constants, (ii) the comparison of the static methods, (iii) the extraction of the lateral photodiode sensitivity from combined dynamic and static techniques, and (iv) the refractive index analysis.

II. EXPERIMENT

All AFM experiments were performed using a MultiMode Picoforce with Nanoscope III controller (Veeco; Digital Instruments, USA), with optical viewing system and signal access module (scanners PF and K; not vertical engage). The cantilevers used were commercial rectangular uncoated tipless silica cantilevers (approximate dimensions: length of 250 μm, breadth of 35 μm) from MikroMasch. A frame grabber from National Instruments, IMAQ-1405 together with IMAQ VISION and LABVIEW were used for capturing images with a charge coupled device (CCD) camera. A National Instruments DAQ card (PCI-MIO-16E) and a LABVIEW program were employed for capturing the thermal vibration, calculating frequency spectra, and fitting peaks to simple harmonic function with added white noise. The AFM is located in a room which is temperature controlled to 20.5 ± 0.5 °C.

A. Normal spring constant calibration

1. Cleveland et al.: Added mass

The attachment of several different masses (M_s) to a cantilever and measuring the corresponding normal resonant frequency enabled the normal spring constant k_v to be determined from the slope of a linear plot of M_s vs $(2\pi f_v)^2$, according to the formula[6]

$$M_s = \frac{k_v}{(2\pi f_v)^2} - m_e. \tag{1}$$

Tungsten spheres of different sizes were adhered to the cantilevers with a Micromanipulator 5171 (Eppendorf AG, Germany). The size of each sphere was determined with image analysis of images grabbed with a 50× objective on the Nikon Optiphot-100S microscope. The image analysis algorithm employed edge detection on eight spots around the sphere and then a circular fit giving the diameter of the particle. Four different particles were used for each cantilever. Both the torsional and normal resonance frequencies were detected as follows. The cantilever was mounted in the AFM and allowed to vibrate freely due to thermal motion. The photodetector signals for the normal and torsional signals were grabbed with a DAQ card and analyzed in the Fourier domain to find the resonance frequency. To reduce the noise in the frequency spectra, 500 individual spectra were averaged into one average frequency spectrum. The average frequency spectrum close to the fundamental resonance peak was fitted to a single harmonic function with added white

noise to calculate the resonant frequency and Q factor for the peak.

2. Sader et al.: thermal vibrations

The cantilever is allowed to vibrate freely due to thermal motion in a fluid such as air. The frequency and Q factor of the fundamental resonance are used together with the dimensions (length l and breadth b) of the cantilever, the density ρ and viscosity η of the fluid. These parameters are then used to calculate the normal spring constant[7]

$$k_v = 0.1906 \rho b^2 l Q_v (2\pi f_v)^2 \Gamma_i^v(\mathrm{Re}_v), \tag{2}$$

$$\mathrm{Re}_v = \frac{\rho b^2 2\pi f_v}{4\eta}, \tag{3}$$

$\Gamma_i^v(\mathrm{Re}_v)$ is the imaginary component of the hydrodynamic function for normal vibrations described in Ref. 17.

The dimension of the cantilevers was measured with an Optical microscope, Nikon Optiphot 100-S, with 20× and 50× objectives, respectively, for length and breadth. Images were grabbed with a CCD camera and analyzed in National Instrument IMAQ VISION ASSISTANT 7.1. Resonant frequencies and Q factor were obtained as above.

The method by Sader *et al.* gives the spring constants for the full free length of the cantilevers. The other methods used in this work give the spring constants at the position where the calibration has been done, i.e., a few micrometers from the free end of the cantilever.[12,18] The results of the normal Sader method are thus recalculated according to

$$k_v = k_v^{\ell}\left(\frac{l}{l-\Delta l}\right)^3, \tag{4}$$

where a value of 10 μm was used for Δl.

B. Torsional photodetector calibration

First a cantilever was mounted in the AFM head and the laser and detector were aligned, the cantilever was removed, and a mirror was mounted on the scanner to reflect the laser onto the detector. A three-leg scanner was used to tilt the AFM head. Small changes in the angle were achieved with the built-in step motor; the actual tilt was determined optically as follows. A camera was mounted with a view of an edge on the back of the AFM head. Images were grabbed to monitor the real movement of the head as it was tilted with the step motor. The tilt angle applied was then calculated on geometrical considerations after image processing (edge detection on the position change of the AFM head) of these images. The detector signals—both normal and torsional—were grabbed with a DAQ card from National Instruments.

C. Torsional spring constant calibration

1. Cleveland et al.: Added mass

The change in torsional resonance frequency due to added mass is determined analogously to the normal case.[12] In this case r is the radius of the attached sphere and ρ_s is its density.

$$\frac{28\pi\rho_s r^5}{15} = \frac{k_\phi}{(2\pi f)^2} - J_e. \tag{5}$$

The torsional spring constant k_ϕ is determined from the slope of a linear plot of $28\pi\rho_s r^5/15$ vs $(2\pi f_v)^2$. The sphere radius was determined as above.

2. Sader et al.: Thermal vibration

Analogously to the normal method, the torsional[12] approach returns the torsional spring constant according to

$$k_\phi = 0.1592 \rho b^4 l Q_t (2\pi f_t) 2\Gamma_i^t(\mathrm{Re}_t), \tag{6}$$

$$\mathrm{Re}_t = \frac{\rho b^2 2\pi f_t}{4\eta}. \tag{7}$$

$\Gamma_i^t(\mathrm{Re}_t)$ is the imaginary component of the hydrodynamic function for torsional vibrations described in Ref. 19.

The torsional constant was recalculated for the appropriate length by

$$k_\phi = \frac{k_\phi^{\ell} l}{l-\Delta l}. \tag{8}$$

The calibration by Sader *et al.* is partly sensitive to variation in temperature and probably on different humidities since the Q factor is somewhat sensitive to theses parameters; therefore it is best to perform this calibration on a set of cantilevers directly after each other and leave the cantilevers aligned under the laser beam for some minutes before measuring the frequency spectra. By following these recommendations the error between different cantilevers can be minimized and one can still calibrate ten cantilevers in approximately 1.5 h.

3. Direct methods

The pivot[11] and lever[13] methods are based on the same principle of using the piezoactuator to provide a turning moment by applying a normal force at a known distance from the cantilever's long axis, though their ways of treating the resulting data differ slightly. They both provide a direct static measurement of the spring constant, measured under similar conditions to those experienced when the cantilever is used to perform friction measurements. The deflection sensitivity α_0 for a load applied at the center of the cantilever is compared to the deflection sensitivity α_L and the lateral or torsional sensitivity β_L when the load is applied at a distance L from the long axis. If δ the detector lateral sensitivity (V/rad) is known then a torsional constant can be obtained. Alternatively as in the lever method,[13] a torsional calibration factor γ(N m/V) can be used to convert volts to torque directly. (Note that in this case the measurement is geometry and instrument dependent.) The various sensitivities and calibration factors are related by the following equation:[11,13]

$$\frac{\alpha_L}{k_v \beta_L \alpha_0} = \frac{\delta}{k_\phi} L = \frac{L}{\gamma}. \tag{9}$$

In the pivot method,[11] a linearization plot of $[\alpha_L/(k_v\beta_L\alpha_0)]$ vs L gives k_ϕ linked with δ as the gradient (i.e., $1/\gamma$). Strictly, δ can be determined in a similar way[11] from

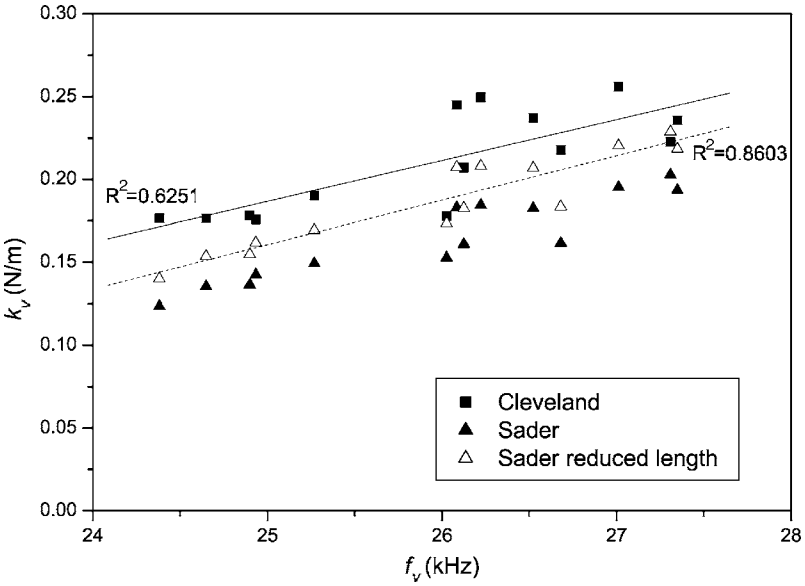

FIG. 1. Normal spring constants for a set of cantilevers (characterized by their resonant frequency) calibrated by the methods of Sader *et al.* and Cleveland *et al.* Values of Sader *et al.* have also been recalculated to a reduced length (from k_v^l to k_v) to enable comparison. The lines are best linear fits to the data of the Cleveland and reduced length Sader methods.

$$\beta_L(1-\alpha_0/\alpha_L)=\frac{L}{\delta}, \tag{10}$$

however, the errors are usually too large to permit this to be done reliably and an independent method is preferred.[10,11]

For the pivot method, a contact mode cantilever tip was glued upside down on a planar substrate and mounted on the piezoscanner. This is henceforth referred to as a pivot. The pivot was then used to twist the tipless cantilever to be calibrated. Force curves were captured (deflection, friction and z sensor) at different points along the width of the cantilever. This was done automatically with a built-in script handling both the positioning and force curve measurements (Autoramp). The positioning in the script used the y offset with an aimed step size of 2 μm. The resulting force curves are then analyzed to calculate α_0, α_L, and β_L, and thus obtain values for γ and k_ϕ. A plot of $1/\beta$ vs L should be linear through the origin, hence the zero position for L was defined such that the line of best fit passed through the origin. The position of the pivot during calibration measurements was recorded with the optical viewing system mounted over the AFM. The resulting images were analyzed to account for nonlinearity of the y movement and obtain the real position of the pivot in relation to the cantilever's long axis. The movement was nonlinear but was extremely well described by a second order polynomial. This corrected L was used for calculations of γ and k_ϕ. The torsional spring constant was calculated with Eq. (9) for pivot method with δ given from the external detector calibration in air.

In the lever method a single value of L is used corresponding to the length of a glass fiber lever glued to the cantilever taken from the central axis. The torsional constant is obtained using the following equation [obtained from Eqs. (9) and (10)],

$$k_\phi=\frac{k_v L^2}{(\alpha_L/\alpha_0-1)}. \tag{11}$$

III. RESULTS AND DISCUSSION

A. Normal spring constant calibration

Figure 1 shows the correlation between measured normal spring constants and the unloaded resonant frequency for 14 rectangular cantilevers obtained using the methods of both Cleveland and Sader. A roughly linear relation between normal spring constant and normal resonance frequency can be observed; this relation has already been described and used elsewhere.[6,15,20] It is clearly seen that the added mass approach systematically generates a slightly higher value for the spring constant than the method of Sader even when the true length is accounted for in the latter method. The agreement is nonetheless reasonably good. We note that a small systematic error of 200 nm in the measurement of the radius of the spheres used for the masses *could* account for such a difference (since the radius is cubed to obtain the mass), though we have no reason to doubt the values of the radii used here. In the comparison presented by Green *et al.*[12] there was remarkably good agreement between calibration methods (much less than 1%) when three rectangular cantilevers covering a large range of spring constants were compared. Given the uncertainty of placement of the spheres in the resonance method a small error would be expected, but this is unlikely to be systematic. The most likely explanation for the small systematic deviation is the fact that the cantilevers are not perfect rectangles—there is a small flangelike protrusion over the last few percent of the cantilever length which means that they do not *perfectly* meet the assumptions of the Sader technique—the width is not technically constant and both the hydrodynamics and the resonance will be marginally different to that of a perfect beam. In the following part of this article we have rather arbitrarily employed the normal spring constant obtained from the method of Sader *et al.*, where this parameter is required in the calculation of torsional spring constants and photodetector sensitivity. This in no way affects the *comparison* of the derived lateral force constants. At this stage we cannot be sure which is the more

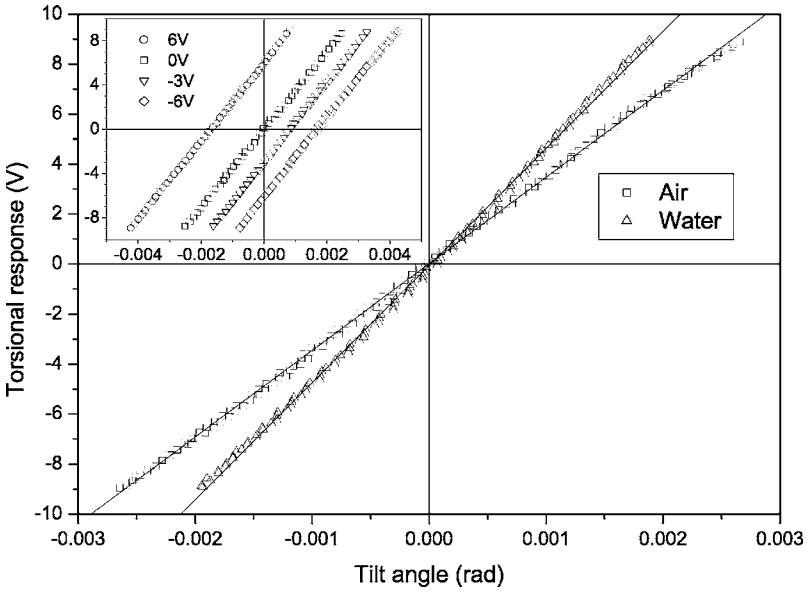

FIG. 2. Detector calibration; torsional detector response as a function of tilt angle for 0 V in normal deflection for air and liquid cell measurements. (The lines are linear best fits to the measured data which return $\delta_{air}=3.52\times10^3$ V/rad and $\delta_{water}=4.67\times10^3$ V/rad.) The insert shows the detector response in air when the laser spot is positioned at different locations at the detector; in the case of no tilt the laser spot was varied from 6 to −6 V in the torsional plane and keeping the normal deflection at 0 V.

reliable, but the relative simplicity of the Sader method makes it the more attractive.

B. Torsional photodetector calibration

The torsional detector response due to lateral tilt of the AFM head (mimicking cantilever twist) is presented in Fig. 2. It can be seen that the detector response is approximately linear with tilt angle over the detector range from −10 to 10 V and the slope of this line is thus the detector sensitivity δ. The two data sets presented in Fig. 2 are measured with a normal deflection signal of 0 V which is a typical value used in measurements; the two data sets were measured in air and in water using a commercial liquid cell. As expected from our optical path calculations,[21] the ratio of the two δ values is dependent on the refractive index of the liquid filling the cell, in this case water ratio is 1.33 (for calculation of the ratio, gradients were obtained from linear fits to three consecutive measurements in each geometry). The significant difference between the δ values for the two cases demonstrates the importance of calibrating for the conditions to be measured. If aqueous measurements are to be performed then the photodetector calibration must be performed with a liquid cell containing liquid of the same index. This fact is not generally appreciated. Note also that a small difference in δ is also expected[21] between measurements performed in *air* if the liquid cell is used or not since the optical path is slightly modified by the glass of the cell. Our measured ratio is 0.96, which agrees well with the calculated value. If, for example, no independent photodetector calibration is made and the γ value is used directly from the force calibration of the cantilever, then this calibration must necessarily be done in the medium to be used or a correction made based on the refractive index and the geometry of the liquid cell employed as done here.

The insert in Fig. 2 shows calibration curves taken at different initial torsional deflection voltages keeping the normal deflection signal constant at 0 V. This, together with similar curves taken at different normal deflection voltages, was conducted to see whether any variation could be expected over different laser spot positions on the detector. The δ values obtained from linear regression taken at various normal deflection voltages are presented in Table I. The two sets of results presented in this table correspond to calibrations performed with the standard cantilever holder in air and also with the initial mirror alignment performed with liquid cell in place, and subsequently removed for the tilting. When changing from a normal "air alignment" to the alignment for liquid cell, it is usually necessary to adjust the position of a mirror employed to direct the laser beam onto the photodetector. The gradients of the slopes are virtually identical in the data set. In neither data set is there any coherent trend with detector position and the maximum scatter of the data in Table I is less than 4%. The difference between the average of each column is negligible, indicating that changes in the mirror position on this scale can be ignored. The results also show that the detector signal is linear over a large range in both normal and torsional deflections and that the laser spot position on the detector does not affect the calibration factor δ.

Cannara *et al.*[14] recently presented a study of the lateral photodetector behavior and concluded that it was extremely nonlinear with laser spot position due to the Gaussian distribution of the laser intensity. In fact, the lateral deflection

TABLE I. Torsional detector sensitivity measured for different normal deflection voltages; set points. δ was measured as in Fig. 2 in air for two setups; the laser aligned on a cantilever in a normal air cell (δ in air) and on a cantilever immersed in water in a liquid cell which necessitated movement of the mirror (δ for tilted mirror).

Set point (V)	δ in air (V/rad)	δ for tilted mirror (V/rad)
−2	3.58×10^3	3.50×10^3
−1	3.60×10^3	3.53×10^3
0	3.52×10^3	3.61×10^3
1	3.57×10^3	3.53×10^3
2	3.58×10^3	3.56×10^3
3	3.54×10^3	3.56×10^3
Average	3.56×10^3	3.55×10^3

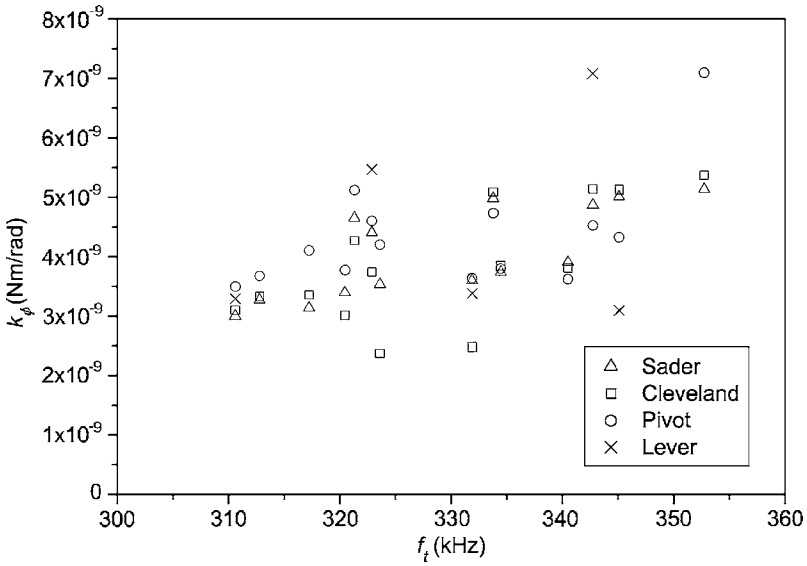

FIG. 3. Torsional spring constants; k_ϕ vs torsional resonance frequency, measured with the following methods: Sader, Cleveand, pivot, lever. The Sader value is that recalculated to a reduced length. In the pivot and lever case, the normal spring constant was first obtained by the Sader method and the externally calibrated value of the torsional detector sensitivity was employed in the pivot case.

sensitivity was well fitted by a parabolic function. This has clear implications for the quantification of the friction force since it becomes more complex when the detector sensitivity response becomes a function of the size of the friction response! However, the results presented here clearly show a different trend and that, at least for the case of our instrument, a linear detector response can be achieved over the entire range of interest for frictional measurements. Thus significant differences occur between different instrumental designs, and analysis as performed here and by Cannara *et al.*[14] is thus crucial for identifying whether the instrument is suited for performing friction force measurements.

We note that our calibration, while rather onerous the first time can be relatively easily repeated, particularly if automated as described here. Ideally, the torsional sensitivity could be extracted from the torsional resonance data as recently proposed[22] and optimized[23] for the normal sensitivity, and we hope to report on this shortly.

C. Torsional spring constant calibration

Despite the fact that a relatively soft ointment was employed for attaching the particles for the torsional Cleveland method, the common feature for all the measurements was a good linear fit to the mass-frequency curves to calculate k_ϕ. Figure 3 presents the torsional calibration results from all the different methods used in this study versus torsional resonant frequency. The trend is less clear than in the case of the normal constant (Fig. 1), though a general increase in k_ϕ with resonance frequency is discernible. All methods return results in the same range, and the scatter within a given data set is of the same order between the methodologies. This is, in fact, a confirmation that all the techniques examined here have approximately the same merit in terms of accuracy and that none (or all!) of them suffer from any systematic error. The fact that the resonance methods agree well with the direct methods is highly reassuring and this is the first time that these methods have been directly compared. No linear fits have been made to the data in order to preserve the figure's clarity, but it is worth noting that were one to do so the coefficients of determination fall in the following order: Sader 0.6, Cleveland 0.5, pivot 0.3, and lever 0.1. This is by no means hard evidence, but tends to suggest that the Sader method is the least prone to error. Since it is also the simplest technique to implement, it would seem reasonable to suggest that this should be the preferred method henceforth.

As mentioned earlier, another approach to quantify friction without direct measurement of k_ϕ is to use the value for γ which can be extracted from the direct (pivot and lever) methods since the torque and photodetector responses can be obtained simultaneously. When doing so, one must be sure to perform the calibration with the same optical path length as subsequently used for the friction measurement itself (see above). In Eq. (10) it can be clearly seen that the accuracy of any determination of δ depends on the difference between unity and the ratio of two measurements which are very close to one another in magnitude, and thus this value is rather unstable at small L. Similarly, the accuracy with which γ can be obtained increases with increasing L. To quantify the reliability with which γ can be obtained and over what values of L, γ was extracted from Eq. (9) (k_ϕ/δ) for the different L values used for the pivot method,[11] and the results are displayed in Fig. 4. The absolute value of L has been used—twisting measurements were, in fact, performed from either side of the cantilever axis as the pivot was ramped across the cantilever. It can be seen that above about 8 μm from the long axis of the cantilever, the data start to plateau out and tend to the same value as the linearized average value. Thus for the cantilevers used in the present study, 8 μm seems to be about the limit for reliable, single point torsion calibrations. Interestingly the trend to zero at small values of L is not a result of inaccuracy in itself—this would rather lead to scatter—but is suggestive of a systematic error. This is likely to be due to the assumption that the cantilever is infinitely thin and that the torque is being applied to a point in plane with the twist axis of the cantilever. In fact, this is not the case since the cantilever has finite thickness (typically of the order of 1 μm), and thus for small L, the approximation becomes progressively more invalid. The γ value obtained using the lever method on this cantilever is also shown using a lever length of 127 μm and good agree-

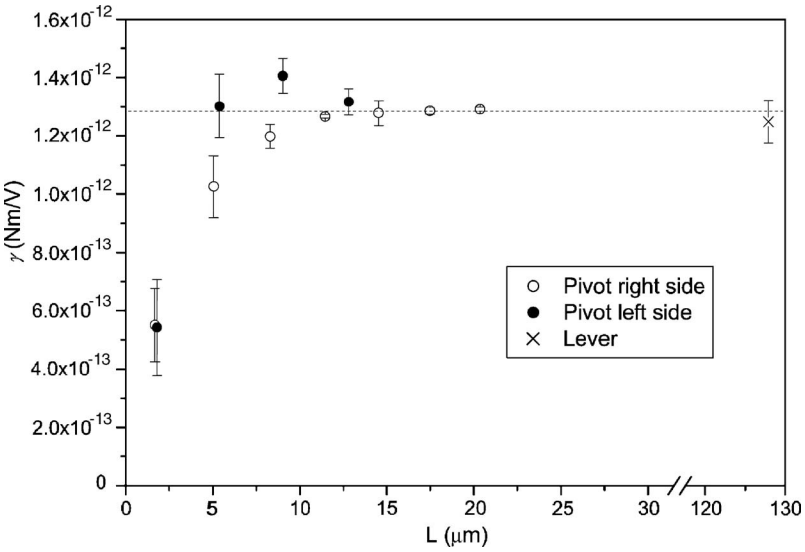

FIG. 4. Torsional calibration factor γ calculated from pivot and lever measurements. Absolute values of L are plotted to superimpose the data from both sides of the cantilever long axis. The dashed line represents the value of γ obtained from the linearization plot from Eq. (9).

ment is observed between this value and the linearized value obtained from the pivot method.

Given the simplicity of the Sader technique for obtaining normal and lateral cantilever spring constants, the major challenge in friction quantification becomes the calibration of the torsional photodetector sensitivity. It is by no means all AFM constructions that lend themselves to the automated tilting procedure employed here, particularly if liquid cells are to be employed. Thus, it is interesting to pursue the possibility of extracting this value by other means. In the description of the pivot method above it can be seen that the data returned by the linearization procedure are the spring constant divided by the torsional sensitivity δ [Eq. (9)]. Thus the direct method can actually be "reverse engineered" to obtain the torsional senstivity if the spring constant can be accurately obtained from a reliable source—such as the Sader method. In Table II we present just such calculated values for ten cantilevers, where k_ϕ is obtained from the Sader method and δ is obtained from γ_{pivot}. The individual δ values have a certain degree of scatter, but the average value $(3.58\times10^3$ V/rad) is extremely close to the value for δ_{air} measured with the external method $(3.56\times10^3$ V/rad). Thus it is possible to obtain a value for δ which agrees well with the externally calibrated one by averaging data obtained from multiple cantilevers and/or several repeat measurements. In this way, the direct pivot approach can instead be used to provide a relatively undemanding means of calibrating the torsional sensitivity.

TABLE II. Calculation of the torsional detector sensitivity in air, according to $\delta=k_\phi/\gamma$, where k_ϕ and γ are obtained by the methods of Sader (reduced length) and (from linearisation plot), respectively.

Sader k_ϕ (Nm/rad)	γ_{pivot} (Nm/V)	δ (V/rad)
3.13×10^{-9}	9.82×10^{-13}	3.19×10^3
3.75×10^{-9}	1.02×10^{-12}	3.68×10^3
4.59×10^{-9}	1.29×10^{-12}	3.56×10^3
3.91×10^{-9}	1.07×10^{-12}	3.66×10^3
4.08×10^{-9}	1.02×10^{-12}	4.01×10^3
5.07×10^{-9}	1.27×10^{-12}	3.99×10^3
5.18×10^{-9}	1.33×10^{-12}	3.90×10^3
3.69×10^{-9}	1.18×10^{-12}	3.13×10^3
4.85×10^{-9}	1.44×10^{-12}	3.38×10^3
3.54×10^{-9}	1.06×10^{-12}	3.34×10^3
	Average	3.58×10^3
	Stdev	0.32×10^3

Equation (10) can strictly be used to obtain δ from the pivot and lever measurements; however, there is large scatter in the results. To quantify this problem we calculated δ using the data in Fig. 4 and the following values were returned: $\delta_{\text{pivot}}=2.6\times10^3$ V/rad and $\delta_{\text{lever}}=5.6\times10^3$ V/rad. There is large discrepancy between these values compared with the value obtained by the independent method Table I, $\delta_{\text{air}}=3.56\times10^3$ V/rad.

Since the reverse calculation gives the same calibration factor as the tilting of the detector, this indicates that such calibrations are robust and of universal application for cantilevers of the same geometry and also independent of the small variations in laser spot location on the cantilever between experiments. Thus, this calibration does not therefore need to be performed for each experiment, but clearly should be performed regularly since the laser response may change slowly with time. In the present study we do not observe any evidence for in-plane bending of the cantilever.[24] The question might also be raised as to whether the detector sensitivity is affected by different sum signals in the detector. We have varied the sum signal by comparing two types of cantilever—one gold coated the other uncoated, but otherwise of identical geometry. In the case of the gold coating, the sum signal on the photodiode was approximately double that of the uncoated cantilevers. Despite this large difference in laser intensity on the detector, we obtain the same torsional calibration factor using the reverse calculation for both the cantilever types, confirming that the calibration is sum signal independent.

IV. CONCLUSIONS

Any residual doubt as to whether the direct, static methods for spring constant measurement return the same value as the dynamic ones are now essentially laid to rest. While

there is rather more scatter in the torsional constants than the normal ones, this probably reflects the fact that the normal constant is prerequisite in obtaining the torsional one which is a rather more involved process. The overall agreement between the techniques is good with the dynamic techniques appearing to have slightly less scatter—the Sader method was marginally more robust. Of the direct methods there appeared to be less scatter in the pivot method.

However, the torsional spring constant is only half the issue since it is actually the lateral photodetector signal which is measured, and this needs to be calibrated in terms of angle. There is no obvious torsional analogy to the so-called sensitivity or constant compliance measurement against a hard substrate for the normal calibration[25] which can be performed *in situ* during the experiment. Thus, it is crucial to calibrate the torsional detector sensitivity for the medium and geometry to be employed in the experiment, and a convenient means of doing so has been presented. We also demonstrate that if the experimental geometries and refractive indices are well known, it is possible to calculate precisely how the sensitivity will change for a given set of conditions which facilitates, for example, performing calibration in air while experiments are performed in liquid. It is still necessary, however, to perform a sensitivity calibration for at least one of the experimental geometries. Thus, one of the advantages of the rather more cumbersome direct methods is that the torsional sensitivity can be extracted from the torsional calibration factor if combined with the torsional spring constant obtained from the Sader method. Since many commercial AFMs are not suited to the direct external method employed here, this observation provides a useful and straightforward means of quantifying lateral force data

The most convenient method to use by far is that of Sader *et al.*, and since it also appears to be the most reliable there would seem to be little reason to employ any other method—though we note that it is not always trivial to access the torsional frequency. For frictional studies in liquid, it would appear most convenient to calibrate both the torsional detector sensitivity and the torsional spring constant in air and then calculate the sensitivity to be employed in the relevant liquid. There is thus no impediment to quantitative measurement of friction with AFM, for example, with the colloid probe technique due to issues of accuracy with calibration of the torsional spring constant and the deflection sensitivity.

ACKNOWLEDGMENTS

The authors acknowledge John Sader for the explanation of the trend in Fig. 4. The AFM was financed by a generous grant from the Knut and Alice Wallenberg foundation. The authors acknowledge a reviewer of the first version of this article for useful comments and bringing Ref. 14 to our attention. One of the authors (T.P.) acknowledges financial support from Swedish Research Council. Two of the authors (M.R. and N.N.) acknowledge support from BiMaC, the Biofibre Materials Centre at KTH and Biomime, the Swedish Centre for Biomimetic Fibre Engineering. One of the authors (M.R.) is a fellow of the Swedish Research Council.

[1] W. A. Ducker, T. J. Senden, and R. M. Pashley, Nature (London) **353**, 239 (1991).
[2] I. C. H. Berg, M. W. Rutland, and T. Arnebrant, Biofouling **19**, 365 (2003); K. Theander, R. J. Pugh, and M. W. Rutland, J. Colloid Interface Sci. **291**, 361 (2005); H. Mizuno, M. Kjellin, N. Nordgren, T. Pettersson, V. Wallqvist, M. Fielden, and M. W. Rutland, Aust. J. Chem. **59**, 390 (2006); J. Stiernstedt, N. Nordgren, L. Wagberg, H. Brumer, D. G. Gray, and M. W.Rutland, J. Colloid Interface Sci. **303**, 117 (2006).
[3] D. H. Gracias and G. A. Somorjai, Macromolecules **31**, 1269 (1998); G. Meyer and N. M. Amer, Appl. Phys. Lett. **57**, 2089 (1990); C. M. Mate, G. M. McClelland, R. Erlandsson, and S. Chiang, Phys. Rev. Lett. **59**, 1942 (1987); R. W. Carpick and M. Salmeron, Chem. Rev. (Washington, D.C.) **97**, 1163 (1997).
[4] Y. H. Liu, T. Wu, and D. F. Evans, Langmuir **10**, 2241 (1994).
[5] J. E. Sader, Rev. Sci. Instrum. **66**, 4583 (1995); T. J. Senden and W. A. Ducker, Langmuir **10**, 1003 (1994); J. M. Neumeister and W. A. Ducker, Rev. Sci. Instrum. **65**, 2527 (1994); J. L. Hutter and J. Bechhoefer, *ibid.* **64**, 1868 (1993).
[6] J. P. Cleveland, S. Manne, D. Bocek, P. K.Hansma, Rev. Sci. Instrum. **64**, 403 (1993).
[7] J. E. Sader, J. W. M. Chon, and P. Mulvaney, Rev. Sci. Instrum. **70**, 3967 (1999).
[8] Y. H. Liu, D. F. Evans, Q. Song, and D W. Grainger, Langmuir **12**, 1235 (1996); J. L. Hazel and V. V. Tsukruk, Trans. ASME, J. Tribol. **120**, 814 (1998); J. L. Hazel and V. V. Tsukruk, Thin Solid Films **339**, 249 (1999); O. Pietrement, J. L. Beaudoin, and M. Troyon, Tribol. Lett. **7**, 213 (1999); S. Jeon, Y. Braiman, and T. Thundat, Appl. Phys. Lett. **84**, 1795 (2004); S. Jeon, Y. Braiman, and T. Thundat, Rev. Sci. Instrum. **75**, 4841 (2004); N. Morel, M. Ramonda, and P. Tordjeman, Appl. Phys. Lett. **86**, 163103 (2005).
[9] D. F. Ogletree, R. W. Carpick, and M. Salmeron, Rev. Sci. Instrum. **67**, 3298 (1996); M. Varenberg, I. Etsion, and G. Halperin, *ibid.* **74**, 3362 (2003).
[10] R. G. Cain, M. G. Reitsma, S. Biggs, and N. W. Page, Rev. Sci. Instrum. **72**, 3304 (2001); R. G. Cain, S. Biggs, and N. W. Page, J. Colloid Interface Sci. **227**, 55 (2000); E. Liu, B. Blanpain, and J. P. Celis, Wear **192**, 141 (1996).
[11] G. Bogdanovic, A. Meurk, and M. W. Rutland, Colloids Surf., B **19**, 397 (2000).
[12] C. P. Green, H. Lioe, P. Mulvaney, and J. E. Sader, Rev. Sci. Instrum. **75**, 1988 (2004).
[13] A. Feiler, P. Attard, and I. Larson, Rev. Sci. Instrum. **71**, 2746 (2000).
[14] R. J. Cannara, M. Eglin, and R. W. Carpick, Rev. Sci. Instrum. **77**, 053701 (2006).
[15] J. Ralston, I. Larson, M. W. Rutland, A. A.Feiler, and M. Kleijn, Pure Appl. Chem. **77**, 2149 (2005).
[16] S. S. Perry, MRS Bull. **29**, 478 (2004).
[17] J. E. Sader, J. Appl. Phys. **84**, 64 (1998).
[18] J. E. Sader, I. Larson, P. Mulvaney, and L. R. White, Rev. Sci. Instrum. **66**, 3789 (1995).
[19] C. P. Green and J. E. Sader, J. Appl. Phys. **92**, 6262 (2002).
[20] A. Feiler, M. A. Plunkett, and M. W. Rutland, Langmuir **19**, 4173 (2003).
[21] See EPAPS Document No. E-RSINAK-78-039709 for a document indicating how the optical path length affects the calbration parameters. This document can be reached via a direct link in the online article's HTML reference section or via the EPAPS homepage (http://www.aip.org.pubservs.epaps.html).
[22] M. J. Higgins, R. Proksch, J. E. Sader, M. Polcik, S. McEndoo, J. P.Cleveland, and S. P. Jarvis, Rev. Sci. Instrum. **77**, 013701 (2006).
[23] P. Attard, T. Pettersson, and M. W. Rutland, Rev. Sci. Instrum. **77**, 116110 (2006).
[24] J. E. Sader and C. P. Green, Rev. Sci. Instrum. **75**, 878 (2004).
[25] M. W. Rutland, J. W. G. Tyrrell, and P. Attard, J. Adhes. Sci. Technol. **18**, 1199 (2004).